S.D. Hoath, O.G. Harlen, I.M. Hutchings, Jetting behaviour of polymer solutions in drop-on-demand inkjet printing. Journal of Rheology 2012.

Jetting behaviour of polymer solutions in drop-on-demand inkjet printing

Stephen D. Hoath

Department of Engineering, Inkjet Research Centre, University of Cambridge, IfM, 17 Charles Babbage Road, Cambridge, CB3 0FS, United Kingdom

Oliver G. Harlen

Department of Applied Mathematics, School of Mathematics, University of Leeds, Leeds, LS2 9JT, United Kingdom

Ian M. Hutchings

Department of Engineering, Inkjet Research Centre, University of Cambridge, IfM, 17 Charles Babbage Road, Cambridge, CB3 0FS, United Kingdom

Synopsis

The jetting of dilute polymer solutions in drop-on-demand printing is investigated. A quantitative model is presented which predicts three different regimes of behaviour depending upon the jet Weissenberg number Wi and extensibility of the polymer molecules. In regime I (Wi < ½) the polymer chains are relaxed and the fluid behaves in a Newtonian manner. In regime II (½ < Wi < L) where L is the extensibility of the polymer chain the fluid is viscoelastic, but the polymer do not reach their extensibility limit. In regime III (Wi > L) the chains remain fully extended in the thinning ligament. The maximum polymer concentration at which a jet of a certain speed can be formed scales with molecular weight to the power of (1-3ν), (1-6ν) and -2ν in the three regimes respectively, where ν is the solvent quality coefficient. Experimental

data obtained with solutions of mono-disperse polystyrene in diethyl phthalate with molecular weights between 24 - 488 kDa, previous numerical simulations of this system, and previously published data for this and another linear polymer in a variety of "good" solvents, all show good agreement with the scaling predictions of the model.

I. Introduction

It has long been recognised that the addition of long chain macromolecules, even at low concentrations, can dramatically affect the break-up of liquid jets generated by flow through a nozzle (Goldin *et al* (1969), Hoyt *et al* (1974), Hinch (1977), Goren and Gottlieb (1982), Mun *et al* (1998), Christanti and Walker (2001), Anna and McKinley (2001), Basaran (2002), McKinley and Sridhar (2002), Tuladhar and Mackley (2008), Vadillo *et al* (2011)). The high extensional strains in these flows mean that the presence of polymers can significantly delay jet break-up even at concentrations well below c^*, the overlap concentration. For example, Clasen *et al* (2006) showed that the minimum concentration c_{min} at which a polymer will delay capillary break-up is smaller than c^* by a factor of order $1/L^2$ (where L is the extensibility of the polymer, defined as the ratio of the full contour length to the diameter of gyration at equilibrium).

Polymer solutions are often used in ink-jet printing for industrial and research applications, and there is a need to predict their behaviour. High molecular weight polymer, included deliberately or as a result of contamination or poor quality control, can seriously affect the reliability of jetting. Nominally identical fluids with the same behaviour in low shear viscosity tests can nevertheless exhibit dramatically different printing performance. Knowledge of the origin of these effects is essential for quality

control and to improve printing reliability. However, current guidelines on the effects of different polymer concentrations and molecular weights on jet behaviour are based upon rough 'rules of thumb' rather than on more fundamental understanding.

The break-up of jets of viscoelastic fluids in drop-on-demand (DoD) ink-jet printing has been studied both experimentally (Meyer *et al* (1999), Bazilevskii *et al* (2005)) and by numerical simulation (Morrison and Harlen 2010). These studies were all performed with a fixed level of stimulus applied to the print-head actuator. At low concentrations, high molecular weight polymers are beneficial in preventing satellite drop formation, although at the expense of lower jet speeds. However, at higher concentrations the main drops fail to detach and can even be drawn back towards the nozzle. Thus for a particular level of drive stimulus there is a critical polymer concentration at which jetting fails completely. Successful printing generally requires a prescribed drop speed, and so it is valuable to determine the threshold polymer concentration at which printing at this speed is possible, with the maximum available print-head drive.

de Gans *et al* (2004) determined this 'jettability' threshold for solutions of polystyrene with different molecular weights in acetophenone. They found that for molecular weight, M_w, in the range 564-2530 kDa, the maximum tolerable concentration of polymer was well below c^*, and apparently scales as $M_w^{-2.14}$, suggesting that the viscoelastic stresses caused by the extensional flow in the jet are responsible for limiting the maximum achievable jetting speed.

Other studies [Hoath *et al* (2009) and Hoath *et al* (2007)] determined limits to jetting for diethyl phthalate solutions of polystyrene with different molecular weights, for a Xaar XJ126-200 industrial print-head, in terms of the length of the ligament

formed behind the ejected drop, for main drop speeds of ~ 6 m s^{-1}, but the 'jettability' threshold in this system apparently scales as ~ M_w^{-1} for higher M_w.

The aim of the present work is to determine practical rules to establish drop-on-demand jetting limits for polymer solutions, and to compare the scaling laws with model predictions. This paper presents new experimental results for the limits to jetting of solutions of mono-disperse linear polystyrene in a good solvent, diethyl phthalate. Although the polymers used in practical ink formulations are rarely linear and are typically present at higher concentrations (e.g. Xu *et al* 2007), a model system was chosen that would readily allow the results to be interpreted in terms of the polymer chain length. This system has been extensively characterised in previous rheological studies (Clasen *et al* (2006), Vadillo *et al* (2010)) and can be described by the Zimm model. This allows us to relate the rheological behaviour to the concentration and molecular weight of the polymer. From this we are able to show, by using a simple model for jetting, how threshold concentration for jetting varies with molecular weight. We also reinterpret the results of de Gans *et al* (2004) and previous numerical simulation results [Morrison & Harlen (2010)], with the help of this simple model.

II. Simple Model of Jetting

A. Constitutive Model

A simple constitutive model for the rheological properties of dilute polymer solutions is the multimode FENE-CR model [Chilcott and Rallison (1988)]. In this model the stress is given by

$$\boldsymbol{\sigma} = 2\eta_s \mathbf{E} + \sum G_i f_i (\mathbf{A}_i - \mathbf{I}) \qquad (1)$$

where $2\eta_s\mathbf{E}$ is the viscous stress contributed by the solvent, G_i is the elastic modulus of the i-th mode with $\mathbf{A}_i$ the corresponding conformation tensor and f_i a nonlinear function that enforces finite extensibility,

$$f_i = \left(1 - tr(\mathbf{A}) / L_i^2\right)^{-1}. \tag{2}$$

with L_i the extensibility of the i-th mode. Each conformation tensor $\mathbf{A}_i$ evolves as

$$\overset{\nabla}{\mathbf{A}}_i = -\frac{f_i}{\tau_i}(\mathbf{A}_i - \mathbf{I}), \tag{3}$$

where τ_i is the relaxation time of the i-th mode and $\overset{\nabla}{\mathbf{A}}_i$ denotes the upper convected derivative of $\mathbf{A}_i$. For the polystyrene solution the model parameters L (finite extensibility), G (shear modulus) and τ (relaxation time) can be determined from the Rouse-Zimm spectrum [Clasen *et al* (2006), Morrison and Harlen (2010)] in terms of the weight fraction c and molecular weight M_W of the polymer and the solvent quality coefficient v. (The value of the solvent quality coefficient v lies between 0.5 and 0.6.) The elastic moduli G_i are equal (to G) for each mode and given by

$$G_i = \frac{cRT}{M_w} \tag{5}$$

where c is the concentration of polymer, and so are inversely proportional to molecular weight. The remaining parameters depend upon the equilibrium polymer coil size, R_g, which scales as M_w^{ν} [Clasen *et al* (2006)]. The relaxation times are related by

$$\tau_i = \frac{\tau_1}{i^{3\nu}} \quad \text{with} \quad \tau_1 \approx \frac{\eta_s R_g^{\,3}}{k_B T} \propto \eta_s M_w^{\,3\nu} \tag{6}$$

while the extensibilities L_i are related by

$$L_i = \frac{L}{i^{\nu}}, \tag{7}$$

with L equal to the ratio of the maximum length of the polymer chain, l to its equilibrium diameter.

$$L \approx \frac{l}{2R_g} \propto M_w^{1-\nu}. \tag{8}$$

This model assumes that the chains behave independently so that $c < c^*$ where c^* is the critical concentration for overlap. There is some debate on the precise definition of c^*, which corresponds roughly to the concentration at which the polymer contribution to the zero shear viscosity becomes significant. Graessley (1980) provides a definition that is 77% of the other value commonly used, as discussed by Clasen *et al* (2006); we follow Graessley (1980) and thus use a conservative estimate for the present work.

The Zimm model predictions for the relaxation times apply strictly only to dilute polymer solutions in linear response. However, molecular dynamics simulations by Hsieh and Larson (2005) show that significant coil-stretch hysteresis only occurs for polystyrene in theta solvents and molecular weights above 500 kDa. Clasen *et al* (2006) find that Zimm model predictions of the extensional relaxation time in capillary thinning under-estimate their results for high molecular weight semi-dilute polystyrene solutions. These results have been confirmed by recent measurements of extensional relaxation times in low viscosity fluids, e.g. Campo-Deaño and Clasen (2010), and Ardekani *et al* (2010). Indeed Vadillo *et al* (2012) have just reported a very significant enhancement of the extensional relaxation time for polystyrene (PS) in diethyl phthalate (DEP) at molecular weights of ~ 100 kDa, which is directly relevant to the present work. Consequently the Zimm relaxation time is likely to be an under-estimate of the true relaxation time.

Similarly, recent experiments to determine the value of extensibility, L, by Szabo *et al* (2012) using a falling plate technique suggest that in practice this is significantly shorter than molecular theory would suggest. However, these

experiments were performed with much higher molecular weight polystyrene than that considered here.

B. Model for drop-on-demand jetting of polymer solutions

Viscoelastic effects would be expected to affect jettability when the relaxation times are longer than the timescales for the jetting process. The length of the actuation pulse is typically around 20 μs, which is roughly equal to the Rayleigh break-up time $\sqrt{(\rho R^3/\gamma)}$ for a 25 μm radius nozzle. In polymeric fluids the final stages of break-off are controlled by an elasto-capillary balance in which the radius decays exponentially with an e-folding time of $3\tau_1$ until the polymer chains become fully extended [Entov and Hinch (1997), Clasen *et al* (2006)]. However, although these timescales affect the way in which the drops and ligaments break up, they are not responsible for controlling the velocity of the ejected drop. The final drop velocity is instead controlled by the degree to which the drop is decelerated by the stretching force in the ligament of fluid behind the main drop prior to break-off.

In this section we present a simple model to determine the degree to which the fluid ligament slows down the main drop, once it has issued from the nozzle, based upon a similar approach outlined by Bazilevskii *et al* (2005). Gravity can be neglected on DoD length scales. As shown in Figure 1 (based upon Figure 7 of Bazilevskii *et al* (2005)), during this phase we assume that the jet consists of a main drop of volume V_{drop} that has issued from a nozzle of diameter D at initial speed U_0. The drop is connected to the fluid meniscus by a ligament of fluid of volume V_{lig} with an initial length d, which for simplicity we shall take to be equal to the nozzle diameter D.

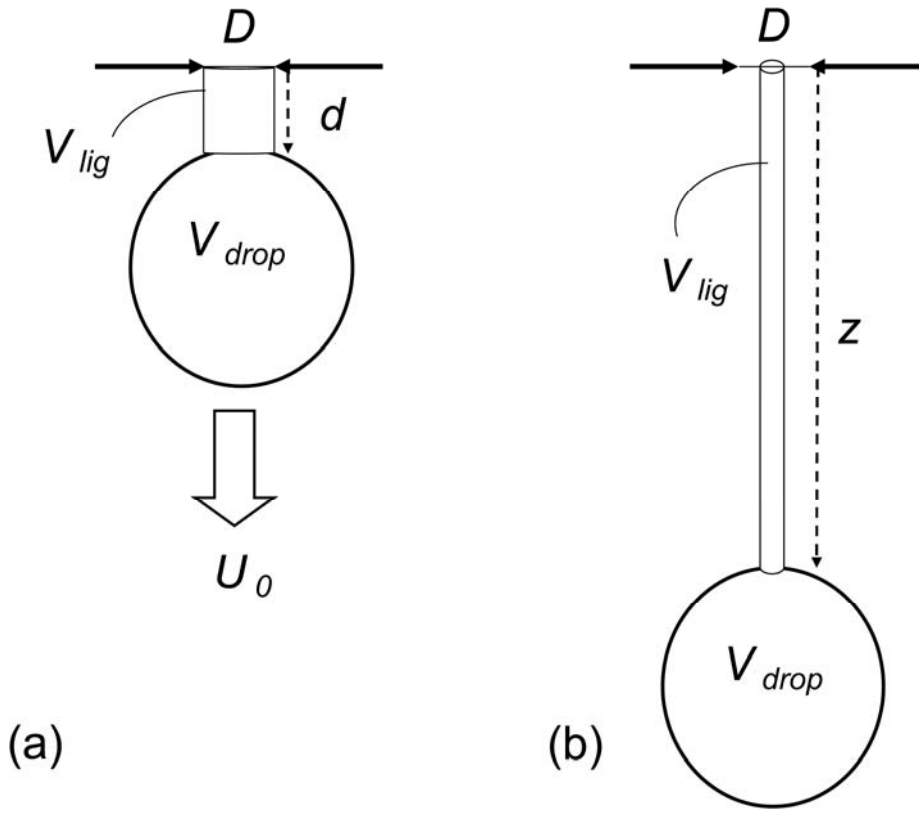

Figure 1. Model of a stretching ink-jet ligament, following Bazilevskii *et al* (2005). Ligament volume is conserved as the ligament stretches from initial length d to z, as depicted in (a) and (b). The main drop speed in (a) is U_0 and in (b) has fallen to U.

At this time the actuation pulse has completed and so the fluid in the nozzle is effectively at rest, and the ligament is subject to an initial extension rate of U_0/d. In the subsequent motion we assume that both the ligament and drop volumes remain constant, and that the ligament deforms uniformly.

On the assumption that the only forces acting on the drop are from the stress difference in the ligament, the drop velocity satisfies

$$\rho V_{drop}\frac{dU}{dt} = -\frac{V_{lig}}{z}\left[3\eta_s\frac{U}{z} + \sum G_i f(A_{i\,zz} - A_{i\,rr})\right]. \qquad (9)$$

where the tensor components from equation (3) are given by,

$$\frac{dA_{i\,zz}}{dt} = \left(\frac{2U}{z} - \frac{f_i}{\tau_i}\right)A_{i\,zz} + \frac{f_i}{\tau_i}$$
$$\frac{dA_{i\,rr}}{dt} = -\left(\frac{U}{z} + \frac{f_i}{\tau_i}\right)A_{i\,rr} + \frac{f_i}{\tau_i} \quad . \tag{10}$$

The initial Weissenberg number is given by Wi = $U_0\tau_1/d$ so that when the ligament is of length z, the effective Weissenberg number has reduced to $U\,\tau_1/z$, where $U = dz/dt$ is the drop speed. Hence if the initial Weissenberg number Wi < ½ the flow is not strong enough to deform the polymer chains from their equilibrium configuration and the fluid behaves as a Newtonian fluid with viscosity (assuming Graessley's factor of 0.77) of

$$\eta_0 = \eta_s + \sum G_i\tau_i = \eta_s(1 + (1/0.77)c/c^*) \quad .$$

Hence equation (9) reduces to

$$\frac{dU}{dt} = -\frac{V_{lig}}{\rho V_{drop}}\frac{3\eta_0 U}{z^2}$$

and integrating from $z = d$ to ∞ gives

$$-\Delta U = \frac{3\eta_0 V_{lig}}{\rho V_{drop} d},$$

The maximum concentration is thus determined by the increase in viscosity and so scales as $cM_w^{(3\nu-1)}$. We shall refer to this low Weissenberg number regime as regime I. However, if Wi > ½ then the initial velocity gradient is sufficient to begin stretching the polymer chains, which will continue to stretch until either Wi drops below ½ and the chains relax, or the chains reach their limit of extensibility. The former case was considered by Bazilevskii *et al* (2005) and we shall show that this applies for ½ < Wi < L, whereas for Wi > L the dominant contribution to the retardation of the jet occurs when the chains are fully extended.

Note that we shall assume that the ligament does not pinch-off during the time when the polymeric stress is active in slowing down the drop, since the timescale for break-off is $3\tau_1$ [Entov & Hinch (1997), Clasen *et al* (2006)], which is long compared with the timescale τ_1 for the viscoelastic stresses to decay in the ligament.

Provided $1 << A_{i\,zz} << L_i^2$ then $f_i \approx 1$ then integrating equation (10) (and neglecting the final term on the right-hand side gives) $A_{i\,zz} \approx \frac{z^2}{d^2} e^{-t/\tau_i}$. The value of $A_{i\,rr}$ remain less than unity and so can be neglected and hence in this limit

$$\frac{dU}{dt} = -\frac{V_{lig}}{\rho V_{drop}}\left[3\eta_s \frac{U}{z^2} + \frac{z}{d^2}\sum G_i e^{-t/\tau_i}\right]. \tag{11}$$

Hence integrating this equation from time t where $z = d$ to later times where $z > d$ gives the reduction in the drop velocity as

$$-\Delta U(z) = \frac{V_{lig}}{\rho V_{drop}}\left[3\eta_s\left(\frac{1}{d} - \frac{1}{z}\right) + \frac{1}{d^2}\sum G_i \int_{z=d}^{z} z e^{-t/\tau_i} dt\right] \tag{12}$$

By assuming that $\Delta U/U$ is small and taking the limit $z \to \infty$ we can approximate the integral

$$\int_{z=d}^{z=\infty} z e^{-t/\tau_i} dt = U_0 \tau_i^2, \tag{13}$$

so that

$$-\Delta U = \frac{V_{lig}}{\rho V_{drop} d}\left[3\eta_s + \frac{U_0}{d}\sum G_i \tau_i^2\right]. \tag{14}$$

The dominant contribution to the sum comes from the first mode and has a relative value of $\mathrm{Wi}\frac{G\tau_1}{3\eta_s}$ compared to the solvent contribution, where Wi is the initial value, and so the reduction in jet velocity contributed by the polymer scales as $c\eta_s^2 M_w^{6\nu-1}$.

The key assumption in this approximation is that $A_{i\,zz} << L_i^2$. Since

$A_{i\,zz} \approx \frac{z^2}{d^2} e^{-t/\tau_i}$ then on the assumption that $\Delta U/U$ is small, the maximum value of $A_{i\,zz}$ is $\frac{4U_0{}^2\tau_1^2}{d^2} e^{-2}$ which requires that $U_0\tau_1 << Ld$. Consequently regime II is limited to the range ½ < Wi < L.

At higher Weissenberg number the first mode will become fully extended at $z = Ld$ and so equation (12) is valid only up to this time. For $z > Ld$ the polymer chains are fully extended and so from equation (10)

$$f_1 A_{1\,zz} \approx \frac{2UL_1^2\tau_1}{z} \tag{15}$$

Thus for $z > Ld$, neglecting all other contributions except that from the first mode, equation (9) reduces to

$$\frac{dU}{dt} = -\frac{V_{lig}}{\rho V_{drop}} \frac{2UG_1L_1^2\tau_1}{z^2} \tag{16}$$

Integrating from $z = Ld$ to ∞ gives

$$-\Delta U = \frac{2V_{lig}G_1\tau_1L_1}{\rho V_{drop}d}, \tag{17}$$

which is larger than the contribution from $z = 0$ to Ld by a factor 2Wi/L. Hence in this limit the retardation of the drop mainly occurs when the polymer chains are fully extended, giving an extensional viscosity $\eta_E = 2G_1\tau_1L^2$ that is $2L^2$ times the Newtonian value. However, this value for the extensional viscosity is only achieved after a linear extensional strain of L, which reduces the cross-sectional area by a factor of L. It is worth noting that if this were the viscosity pertained to flow in the nozzle, the fluid would be unlikely to jet successfully because $L >> 1$ for all but the lowest molecular weights.

Thus in this high Wi limit, regime III, the polymer contribution is only a factor L times that for the Newtonian case in regime I , despite the extensional viscosity value for the fluid increasing by the factor L^2. Hence in this limit the reduction in the drop velocity scales as $c\eta_s M_w^{2\nu}$.

We note that this regime III behaviour was actually observed but not reported by Morrison and Harlen (2010) in their simulations of DoD printing with the FENE-CR model. They compared the drop speed as a function of $G\tau/\eta_s$ (called c in their paper) for different Weissenberg numbers for L = 10 and L = 20. At high Weissenberg numbers they found that the drop speed is independent of the polymer relaxation time and that the retarding effect of the polymer increases with increasing extensibility L, but not in proportion to L^2. By comparing their results for L = 10 and L = 20 (shown in figures 6a and 6b of Morrison and Harlen (2010)), we find that the drop speed is in fact a function of $G\tau L$ (cL in the notation of Morrison and Harlen) as predicted by equation (17) and not of η_E. These simulations therefore related to our regime III.

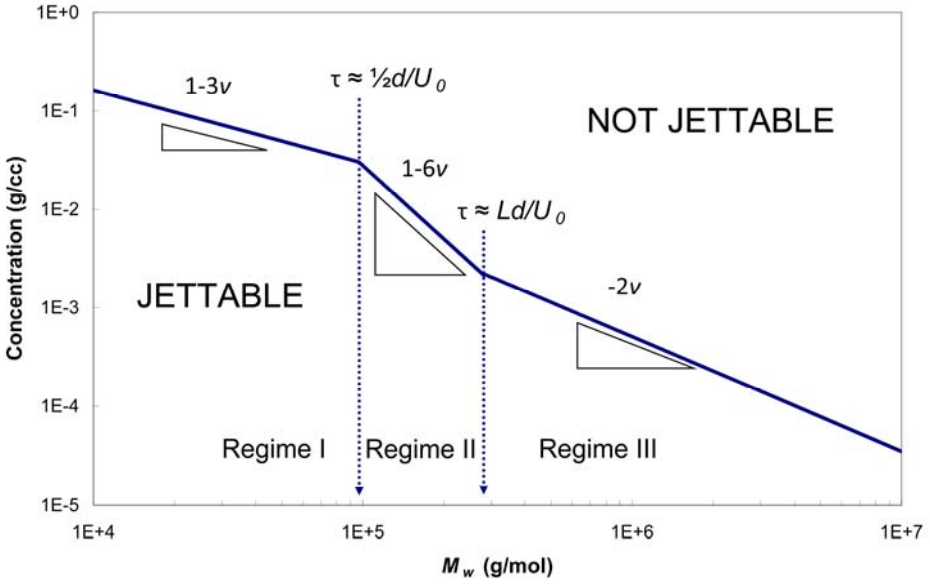

Figure 2. The three regimes (I-III) shown in a plot of maximum polymer concentration for jetting vs. molecular weight M_w, as predicted by the model. Transitions between the regimes occur where polymer relaxation times relate to timescale d/U_0 in the extending jet model, and the transition between regimes II and III depends also on the finite chain extensibility L. The slope in each region is determined by the solvent quality factor v (here assumed to be 0.58). The physical parameters of PS in DEP were used.

Molecular weight scaling laws for DoD jetting of polymers in good solvents can be deduced from these results by assuming that the print-head can provide a fixed impetus to the fluid (corresponding to the maximum drive from the print-head). Then, for the same degree of retardation of the drop, the maximum polymer concentrations will scale as M_w^{1-3v}, M_w^{1-6v} and M_w^{-2v} for regimes I, II and III, respectively, as shown for solvent quality coefficient $v = 0.58$ in the log-log plot of Figure 2. These three scaling laws correspond to whether the zero-shear-rate viscosity, elasticity or high strain-rate extensional viscosity is primarily responsible for the reduction in drop

speed. The M_w values for the transitions between the three regimes are determined from limits derived for the Weissenberg number: from regime I to II, by Wi = $U_0\tau/d \approx$ ½, and from regime II to III by Wi = $U_0\tau/d \approx L$, as shown in terms of τ in Figure 2. Importantly, for extending jets, these transitions depend on jetting conditions such as drop speed and nozzle diameter, polymer characteristics, and the solvent viscosity.

III. Experimental investigation

A. Materials and experimental methods

Samples of mono-disperse polystyrene (PS) with molecular weights M_w between 24 and 500 kDa were obtained from Dow Chemicals and dissolved in DEP (diethyl phthalate: Sigma-Aldrich). The polymers and the designations used here (e.g. PS110 for the polymer with M_w = 110 kDa) are listed in Table I. The polydispersity index M_w/M_n was close to 1.0 for most of the polymers and was <1.15 even for PS488. Also shown in Table I is the critical concentration c^* evaluated for each polymer according to Graessley (1980) and using the intrinsic viscosity data from Clasen *et al* (2006), as described by Vadillo *et al* (2010).

Master solutions were prepared close to the critical concentration c^* and were allowed to equilibrate over a period of two weeks, after which their low shear viscosity η was measured with a controlled strain parallel plate viscometer (Rheometrics ARES), with the results shown in Table I.

designation	M_w	M_n	M_w/M_n	c^* critical concentration wt%	Master solution concentration wt%	η (25ºC) Pa s
PS24	23,800	23,300	1.02	7.0	5.0	0.0242
PS75	75,000	71,000	1.05	3.2	2.7	0.0227
PS110	110,000	104,760	1.05	2.4	2.0	0.0224
PS210	210,000	201,900	1.04	1.52	2.0	0.0236
PS306	306,000	288,680	1.06	1.17	1.3	0.0240
PS488	488,000	443,670	1.13	0.84	1.0	0.0241

Table I: Properties of polymers and of the master solutions (M_w and M_n from supplier).

Further controlled dilutions of these solutions with DEP were prepared to give final concentrations of 100, 200, 400, 1000, 2000, 4000 and 10000 ppm by weight. These diluted fluids had low shear viscosities η only slightly above that of the pure solvent, for which the low shear viscosity $\eta_s \approx 0.010$ Pa s, with the higher concentrations having a low shear viscosity $\eta \approx 0.011$ Pa s. These fluids were prepared in batches and used for jetting experiments after some days to avoid the presence of polymer networks.

The jetting experiments were performed with a Xaar XJ126-200 print-head with a non-wetting nozzle plate, and a shadowgraph imaging technique as described by Hutchings et al (2007) was used to study the jetting behaviour. Xaar PCI+ software was used to control the actuation waveform applied to the print-head. The waveform

shape is usually optimised for each fluid. However, in the present study, the shape of the waveform was kept constant throughout and only the drive amplitude multiplier, denoted by *EFF*, was varied. The Xaar Print-head Commander software could access the range $0.5 < EFF < 1.5$. In these experiments, $EFF = 0.85$ was required to achieve a drop speed of 6 m s^{-1} for pure DEP. Hoath *et al* (2007) investigated the variation of drop speed for polymer solutions ejected at a fixed value of *EFF*: for the concentrations studied, the speed fell below that for the pure solvent in proportion to the polymer concentration. This result (as many others) implies that there is always a limit to the concentration of a polymer solution that can be printed at any desired velocity from a specific ink-jet print-head, since the actuation level *EFF* can only be increased to a certain limit in order to compensate for the liquid's viscoelasticity.

The shadowgraph technique used a High-Speed Photo-Systeme short-duration (20 ns) spark flash light source to provide back-illumination of the ink-jet ligament and drops, synchronised with the arrival of the drops at a point ~ 1 mm from the nozzle exit. Images were captured with a Nikon D70 digital SLR camera (6 megapixel) with a Navitar lens (×12 magnification). The XJ126-200 print-head nozzles were 50 μm in diameter, spaced at a pitch of 137 μm. Figure 3 shows an image of long ligaments of polymer solution generated at 6 m s^{-1}. The jet firing sequence is characteristic of this particular print-head technology, but in this image only eleven of the 126 nozzles are visible. The white vertical scale bar (1 mm long) shows that these long ligaments would span the typical stand-off distance of about 1 mm between the nozzle plane (at the top of the image) and a substrate. Such jets would not normally exhibit successful printing.

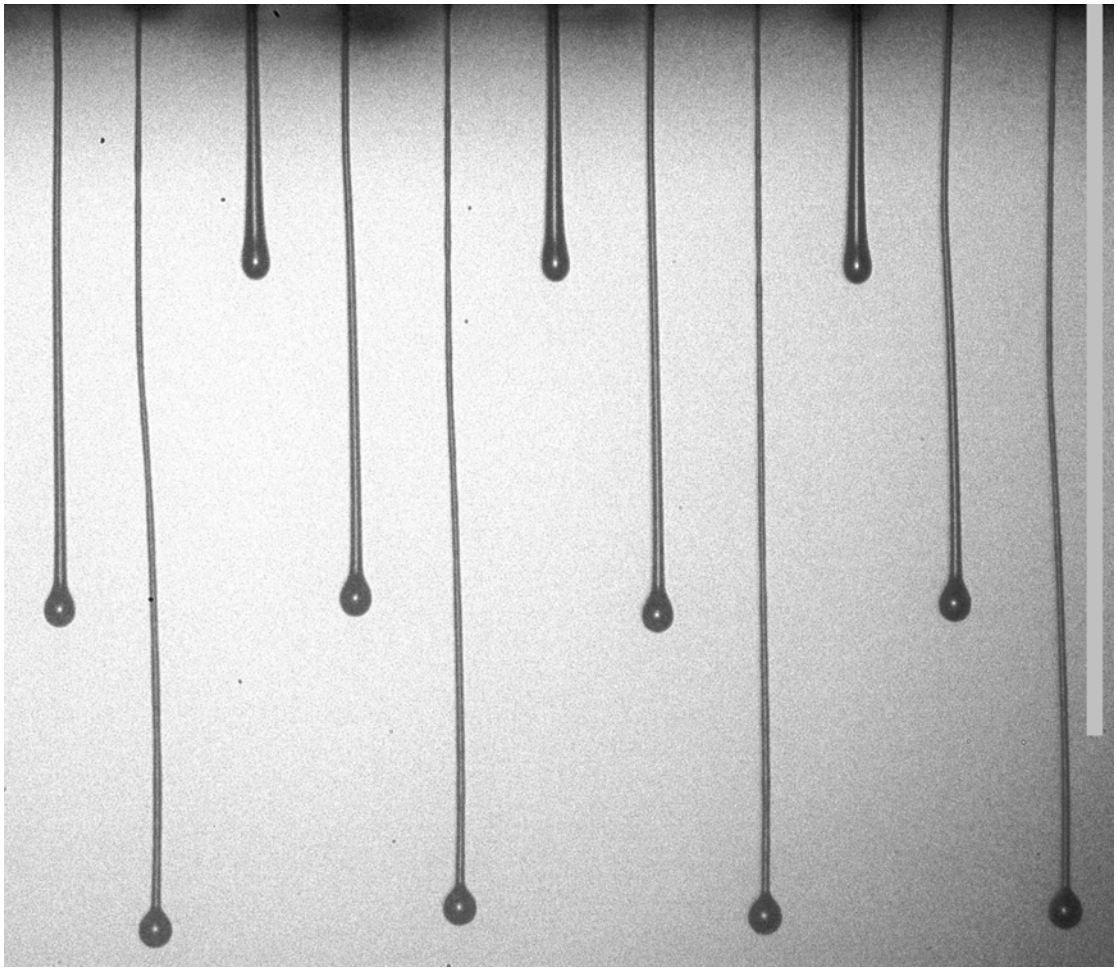

Figure 3. Extra long ligaments with attached drop heads travelling at ~ 6 m s^{-1} as formed by ejecting ~ 0.40 wt% PS210 solution from the Xaar XJ126-200 print-head. The non-wetting nozzle plate is located just above the top edge of the frame and has a nozzle separation of 137 μm horizontally. The vertical scale bar (right) is 1 mm long, to represent the typical "stand-off" distance between the nozzle exit and the substrate.

The velocities of the drops were calculated from measurements of the drop positions from images captured at different flash delay times, averaged over four different images. The length scale was calibrated from the known nozzle pitch and the time was determined to within < 0.1 μs with a delay generator and timer (DG535 and SR620: Stanford Research Systems, USA). The overall uncertainty in measurements of drop speed for jet repetition rates of 500 and 1000 Hz is estimated to be < 0.1 m s^{-1}.

In order to avoid effects from cross-contamination of the print-head in experiments with the different polymer concentrations and molecular weight samples, the pure solvent was first tested and then solutions with increasing polymer concentrations were tested in sequence. Once the maximum concentration for jetting for a particular molecular weight was found, the print-head and fluid reservoir were emptied and cleaned, and the supply tube to the print-head was replaced and flushed with pure solvent through the print-head. Jetting with pure solvent was then performed to check that it would occur at the original value of *EFF* (in essence, to confirm that residual traces of polymer were so slight as to have negligible effect), before the next sequence of solutions was studied. This procedure was followed for all values of molecular weight.

B. Experimental results

Figure 4 shows the values of *EFF* required to produce jets with ~ 6 m s^{-1} drop speed at 1 mm from the nozzle for the polymer solutions with different concentrations and molecular weights. At the lowest concentrations, the *EFF* required for all solutions was indistinguishable from that of the pure solvent (for which *EFF* = 0.85), whereas higher concentrations required higher *EFF* values up to the maximum setting of the print-head drive (*EFF* = 1.50). For all the polymers, the required *EFF* exhibited a near exponential dependence on concentration (*EFF* = 0.85 exp (αc), where the positive constant α depended on the molecular weight of the polymer), and the curves shown in Figure 4 represent fits to this relationship. Although the maximum jettable polymer concentration for a given polymer solvent system depends on the available *EFF* value as well as the required drop speed, the M_w power law slope would be expected to

remain similar. The power law slopes are almost independent of *EFF* value between 1.0-1.5.

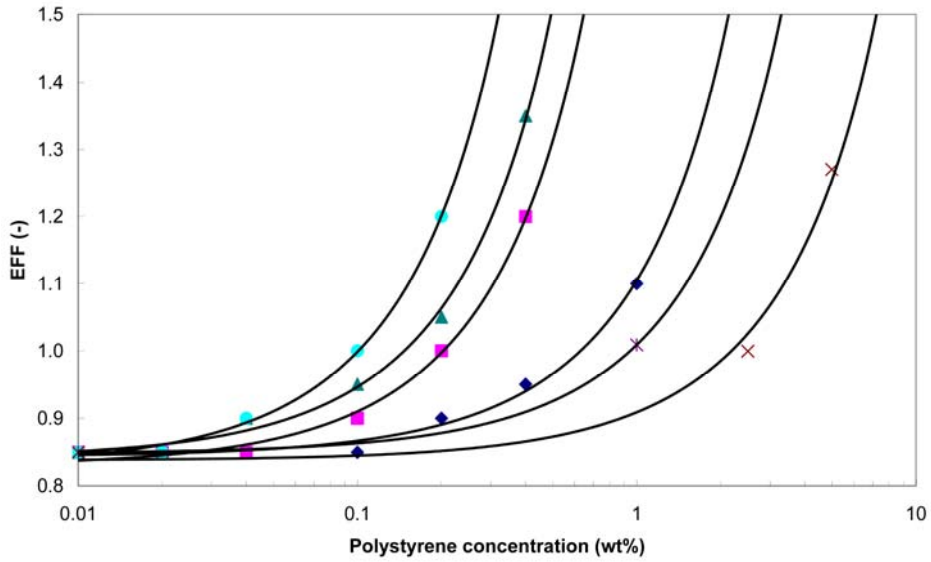

Figure 4. Values of *EFF* producing jets of polystyrene solutions at 6 m s^{-1}, for various molecular weights: PS488 (●), PS306 (▲), PS210 (■), PS110 (♦), PS75 (*) and PS24 (×). The curves represent empirical exponential functions (see text).

The maximum polymer concentrations from the present work, which would produce jets at 6 m s^{-1} with the maximum achievable drive (*EFF* = 1.5), were derived from the exponential curve fits in Figure 4 and shown in Figure 5 as filled squares with error bars reflecting the range of uncertainty in the extrapolation. The only comparable published data for drop-on-demand jetting of mono-disperse polystyrene solutions are those of de Gans *et al* (2004). They used a different, less viscous solvent (acetophenone: ATP) and a slower jetting speed of ~2 m s^{-1}, but the range of molecular weights overlapped that used in the present work and the DoD actuation waveforms had comparable durations in both studies. Figure 5 also shows their data,

extracted from de Gans *et al* (2004) Figure 4 and normalised by the respective values of c^*, plotted as open squares, with errors arbitrarily shown as ± 25%.

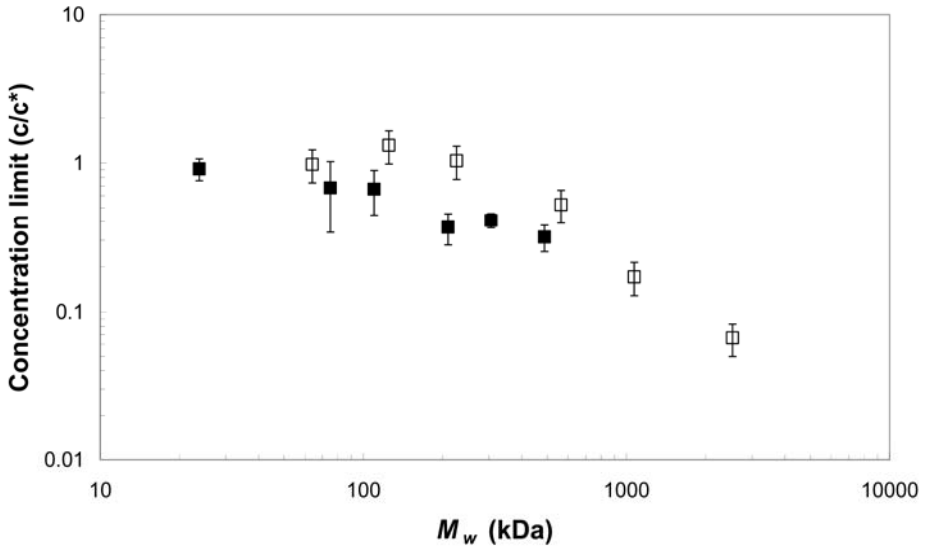

Figure 5: Maximum jettable concentrations c of mono-disperse polystyrene, normalised by c^* and plotted against molecular weight: (■) PS in DEP from the present work; (□) PS in ATP extracted from Figure 4 of de Gans *et al* (2004).

The normalised concentration limits for these two sets of data are in only approximate agreement over the range of molecular weights shown in Figure 5. Although the polymer was the same, the experiments were performed with quite different print-heads and with different solvents, and so some discrepancy in the results would be expected. However, although the normalised concentration limits for the two sets at low molecular weights lie close to $c/c^* \approx 1.0$, the trend in the intermediate molecular weight range (~100 to 500 kDa) is significantly different. de Gans *et al* (2004) described the higher molecular weight dependence of the concentration limit in their data as elastic (or rather, as not viscous) behaviour, but they did not comment on the slope of their data at lower molecular weight. In fact three distinct regimes of polymer behaviour are present in the data sets shown in

Figure 5, which are consistent with the simple jetting model presented in Section 2, as discussed in the next section.

IV. Discussion

The two good solvents for polystyrene [DEP in the present work and ATP for de Gans *et al* (2004)] considered here have similar values of solvent quality factor (v = 0.567 for PS in DEP [Clasen *et al* (2006)] and v = 0.59 deduced from Zimm theory applied to the measured intrinsic viscosity for PS in ATP [de Gans & Schubert (2004)]). However, DEP is significantly more viscous (η_s = 0.010 Pa s) than ATP (η_s = 0.0017 Pa s), and so all relaxation times for PS in the DEP solutions are ~6 times longer than those in ATP for the same M_w.

Zimm parameter	PS in diethyl phthalate	PS in acetophenone
c^*	$M_w^{-0.70}$	$M_w^{-0.77}$
L	$M_w^{0.43}$	$M_w^{0.41}$
G	$c\, M_w^{-1}$	$c\, M_w^{-1}$
τ_1	$(\eta_s = 0.010)\, M_w^{1.70}$	$(\eta_s = 0.0017)\, M_w^{1.77}$

Table II: Scaling of Zimm parameters with M_w and c for relevant solvent parameters.

Table II shows the dependencies of the Zimm model parameters on M_W and c, together with a solvent viscosity multiplier for the (relative) relaxation timescale for polystyrene in these two solvents. Table II is intended to show the relative scaling of parameters for the two polystyrene-solvent systems considered, not their absolute values, which can be deduced from the literature [e.g. Clasen *et al* (2006)].

A. Limits for jetting of polystyrene in DEP

The concentration limits for PS in DEP shown in Figure 5, expressed as the ratio c/c^*, are 0.91±0.15, 0.68±0.32, 0.67±0.22, 0.37±0.09, 0.41±0.05 and 0.32±0.06 for the six molecular weights, in increasing order, studied in this work. Thus the limit for the lowest molecular weights corresponds to $c \approx c^*$. The data points for the lower molecular weights from de Gans *et al* (2004) also lie close to this value. This suggests that for these low molecular weight polymers, jettability is limited by the increase in the fluid's viscosity with increasing polymer content, and not by the effects of viscoelasticity. However, at high molecular weights the limiting concentration c/c^* decreases with increasing molecular weight.

The results for jetting of polystyrene in DEP from a 50 μm diameter nozzle at 6 m s^{-1} are plotted in Figure 6, for molecular weights between 24 and 488 kDa , and those for polystyrene in ATP from a 70 μm diameter nozzle at 2 m s^{-1} [de Gans *et al* (2004)] are shown in Figure 7, for molecular weights between 24 and 2,500 kDa. There are significant differences between the two sets of experimental results which can be interpreted in terms of the model presented in Section II.

The regimes of polymer solution behaviour that are relevant to these two sets of DoD jetting data are clearly different. Figure 6 for PS in DEP at higher M_w is consistent with the behaviour of fully stretched molecules (i.e. regime III). Here, the experiments do not provide evidence of the two transitions, from the Newtonian viscous (regime I) to viscoelastic behaviour (regime II) to fully stretched (regime III), which occur at a low molecular weight.

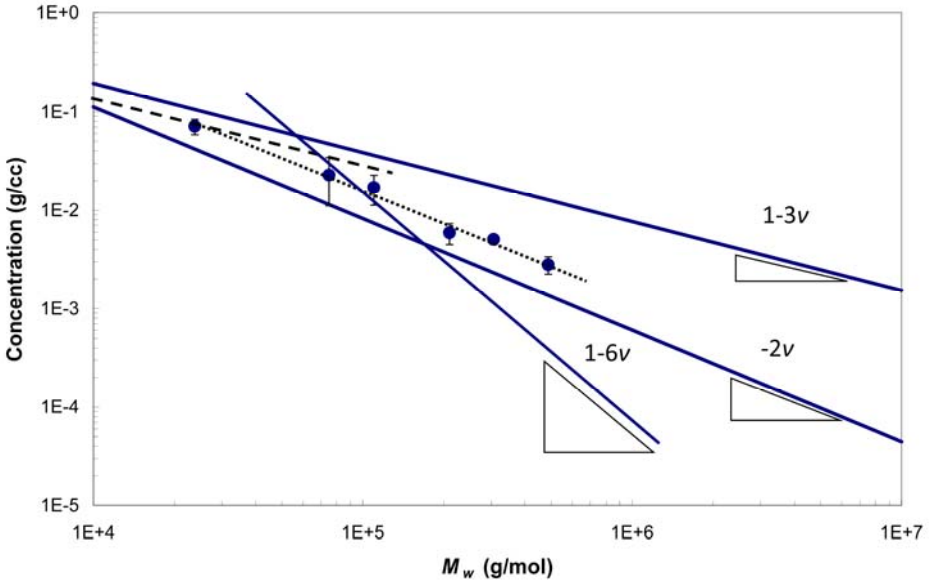

Figure 6. Results from the present experiments for PS in DEP (●), with individual error bars from Figure 4, compared with solid lines with slopes predicted by the model for regime I (1-3ν line), regime II (1-6ν line) and regime III (-2ν line).

The relaxation times τ_1 for polystyrene with M_w from 24 to 488 kDa in DEP can be estimated from the Zimm parameters tabulated by Clasen *et al* (2006) to be 0.4 to 80 μs, corresponding to Weissenberg numbers ranging from 0.5 to 100. (It should be noted that the Zimm time τ_1 used here under-estimates the actual polymer response time as the concentrations c lie within a decade of c^* [Clasen *et al* (2006), Jung *et al* (2011), Vadillo (2012)]). However, rather than as suggested by the position of the regime II line in Figure 6, the lowest M_w of 24 kDa may correspond to the border between regimes I and II.

The data for PS in DEP in Figure 6 show a linear dependence in the log-log plot, with a slope of -1.09 ± 0.04. This matches the slope predicted for regime III behaviour (-1.13 for $\nu = 0.567$) within the experimental error. The same conclusion would be reached if, instead of choosing EFF = 1.5 to determine the limiting concentration from the curves in Figure 4, any other value between 1.0 and 1.5 were

used. For this system, the relatively high solvent viscosity at fast jetting speed result in high Weissenberg numbers even for polymers with modest molecular weights, for which L is small, so that transition from regime I to regime III occurs over a narrow range of molecular weights.

Figure 7 for PS in ATP shows, rather clearly, the previously expected viscous and elastic behaviour (regimes I and II), with the behaviour of the highest molecular weight PS in ATP solution possibly at or even above the transition between regimes II and III.

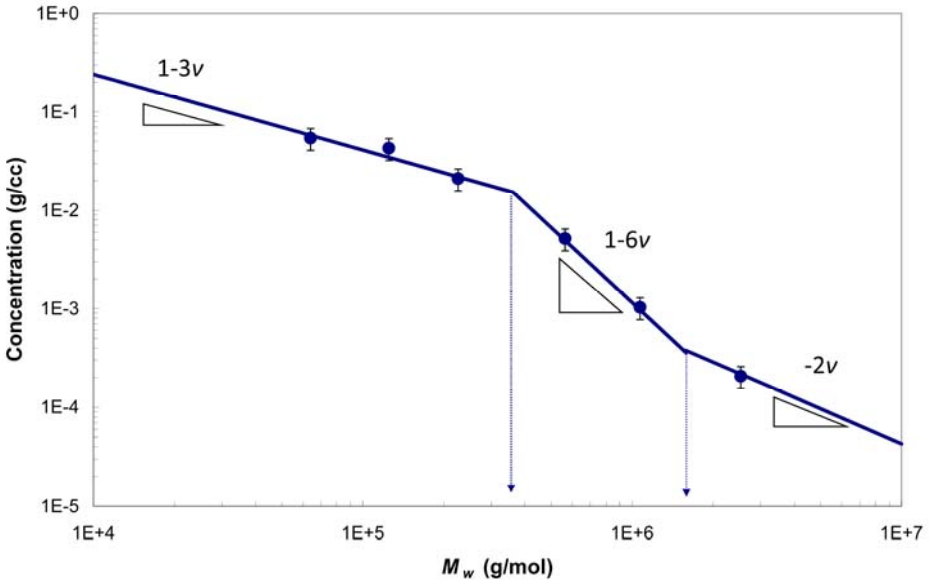

Figure 7. Results from de Gans *et al* (2004) overlaid by theoretical predictions for the jetting behaviour of PS in ATP, with $v = 0.59$ taken from de Gans & Schubert (2004). The predictions have been scaled vertically to achieve a simultaneous fit to the data points in regimes I and III, while the line in regime II was adjusted to fit the rest.

The corresponding Weissenberg numbers for the ATP system (shown in Figure 7) are much lower due to the faster relaxation times, due to lower solvent viscosity, and lower extension rate. The results appear to follow the predictions of the

model for all three regimes, for solvent quality coefficient $\nu = 0.59$. This value of ν is implied by the discussion and measurements quoted by de Gans and Schubert (2004), although the (regime II) power law scaling determined by de Gans *et al* (2004) for higher molecular weights corresponds to a much lower value ($\nu \sim 0.53$).

The transitions between regimes I and II and between regimes II and III are predicted to occur at $2U_0/D = 1/\tau_Z$ and $U_0/D = L/\tau_Z$ respectively. For PS in ATP, the transition from regime II to III corresponds to a molecular weight of ~1500 kDa under the conditions used by de Gans *et al* (2004), close to the upper limit of the molecular weights which they explored. The data point for the highest molecular weight in Figure 7 is therefore likely to lie in regime III. The model predicts that at higher M_w, PS in ATP would certainly lie in regime III under the jetting conditions used in that work. In contrast, under the conditions explored in the present work with DEP as the solvent, the onset of regime III occurred at a molecular weight at least two decades lower: this difference can be accounted for by the lower solvent viscosity, the higher jetting speed, and the smaller nozzle diameter in the present experiments, all of which would affect the transition between regimes II and III.

Figure 8 shows the limits (expressed as c/c*) on jetting of mono-disperse PS and polymethylmethacrylate (PMMA), for a range of molecular weights, in solutions of the good solvent γ-butyrolactone (GBL), taken from Figure 1 of A-Alamry *et al* (2011). The scaling predictions of M_w to the power 0, -3ν and ν-1 appropriate to the 3 model regimes for the c/c^* limits from the present model, with $\nu = 0.55$ and solvent viscosity ~ 0.0017 Pa s for GBL, are overlaid in Figure 8 onto this data.

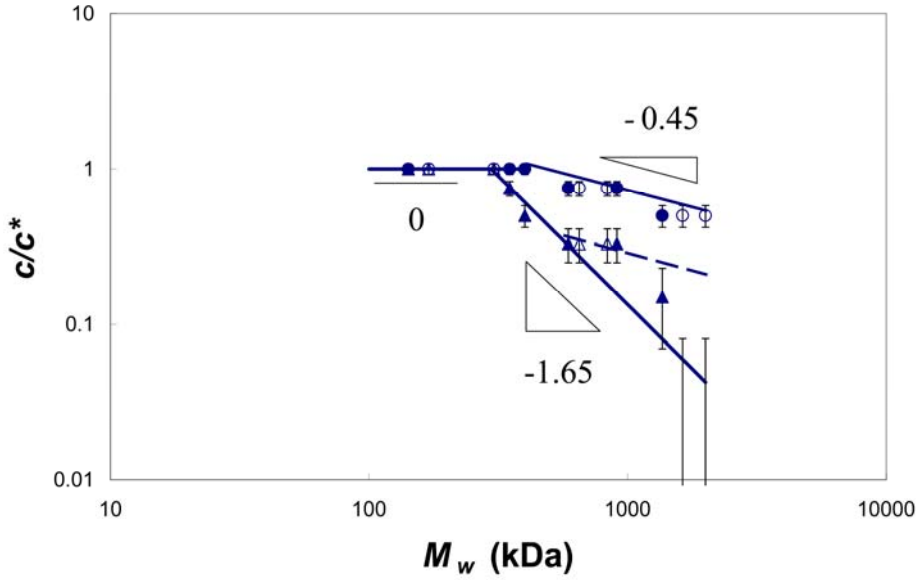

Figure 8. Results taken from Figure 1 of A-Alamry *et al* (2011) for MicroFab jetting behaviour of PS and PMMA solutions in GBL with $v = 0.55$ and solvent viscosity 0.0017 Pa s. Scaling predictions are overlaid to show high M_w behaviour identified as regime II (and? regime III) for 30V drive (▲), and as regime III for 50V drive (●). The data for PMMA are shown by solid symbols; the data for PS by open symbols. (Error bars on this log-log version of the source data represent ± 0.08 in c/c* ratio.)

This comparison provides additional support for our model predictions. The limits for PS and PMMA in the same solvent are almost indistinguishable for the 50 μm diameter MicroFab print head at 30V drive (~3 m/s) and 50V drive (~5.5 m/s). At higher M_w these solutions may follow different regimes of jetting behaviour: regimes II (and then III) at 30V drive and regime III at 50V drive. However, in their paper A-Alamry *et al* (2011) define the limits for "jetting" as being the condition for the ligament to break-off from the nozzle, rather than drop being ejected with a specified speed.

A-Alamry *et al* (2011) also studied jetting of these fluids using a Dimatix DMP print head that has a smaller nozzle diameter and jetted at speeds of ~ 6-10 m/s.

Since this has higher extension rates this would be expected to follow regime III like the higher voltage drive. However, the observed scaling behaviour is appears to closer to regime II. We note that A-Alamry *et al* (2011) found that polymer chain scission occurred within the DMP nozzle which would reduce τ_Z and consequently the *Wi* in the fluid ligament.

B. Further comments

The transition to elastic behaviour with increasing molecular weight at Wi =½ was suggested by Clasen *et al* (2006), whereas the transition to fully extended chain behaviour at Wi = *L* has not been noted before. We have used an average extension rate here rather than a local value, and the emerging jet tip speed is 2-3 times higher than the final drop speed. However, the agreement between the scaling predictions of the model and the experimental data from de Gans *et al.* (2004) and A-Alamry *et al* (2011), including both transitions, and with the trend of the experimental data from the present work within regime III, suggest that the model is well-founded. Morrison and Harlen (2010) reported numerical simulations of the jetting of viscoelastic fluids which also showed the same scaling law as that predicted for regime III.

We can also consider the collapse of the ligaments after break-off. Jet break-off times are delayed on the timescale τ_Z as shown by Hoath *et al* (2009) but ligament collapse (including satellite formation) shows the same order of increased timescales $> \tau_Z$ near c^* for the same polymer solutions in filament stretching experiments [Clasen *et al* (2006)] and in the oblique collision of polymeric jets [Jung *et al* (2011)]. Such effects can only occur in jet formation if the polymer chains remain stretched in flight, and their existence may be taken as further confirmation that this occurs. Studies of viscoelastic drop break-off [Cooper-White *et al* (2002)] support the same conclusion.

The extensional viscosity of a fluid is $\frac{2}{3}L^2$ times that of the same fluid in the Newtonian regime (where Wi < ½) which suggests that if full chain extension occurs inside the nozzle due to the high shear close to the nozzle walls, then jetting from a practical print-head would probably be prevented. This phenomenon could also possibly reduce the effective jet diameter; although the converging fluid flow conditions in most DoD nozzles would tend to roll rather than stretch the polymer chains close to the wall, they can experience the conditions for much longer times than would molecules lying nearer to the jet axis. Other relevant work on the extension of polymer chains in strong extensional flows [e.g. Hinch (1994)] and the influence of solvent quality coefficient on the coil-stretch transition [Somani *et al* (2010)] bear on the underlying polymer physics. Recent experimental studies [Al-Alamry *et al* (2011)] also show that the extensional flow conditions in the jetted ligament can be sufficient to cause chain scission in the polymer.

The results of the present work have important practical implications. We have established some useful and fundamentally-based fluid design rules for polymer solutions. The choice of solvent quality or print head hardware was not critical, but jetting of linear polymers with molecular weights well above 100 kDa while avoiding full stretching is enhanced by choosing a low viscosity solvent and a slow jetting speed, rather than by the use of any particular hardware. Print-head devices with a high maximum drive capability are often desirable, but may produce stretched chains. Solutions of poly-disperse polymers will show jetting behaviour that is restricted by the higher molecular weight components. The limiting concentration for jetting with a solvent quality coefficient v= 0.55 will, in regime I, slowly reduce with M_w, approximately as $M_w^{-0.65}$, while in regime II it reduces more strongly, as $M_w^{-2.3}$, and in regime III rather less strongly, as $M_w^{-1.1}$. This suggests that if jetting occurs in the

viscoelastic regime (regime II) then the behaviour will be most sensitive to the presence of higher M_w components and therefore the polydispersity of the polymer is important, as recently investigated by Yan *et al* (2011) for aqueous PEO jetting.

Studies of the behaviour of non-linear polymer molecules, such as those by Tirtaatmadja *et al* (2006) and Yan *et al* (2011) on low viscosity poly-ethylene oxide (PEO) solutions during drop formation and breakup involve more realistic polymers, but the present model fluids were chosen as more representative of UV curable inks. Yan *et al* (2011) identified a Deborah number limit for the jetting of PEO solutions with 14 kDa < M_w < 1000 kDa, where *De* is the ratio of the effective polymer relaxation time to the characteristic time based on nozzle radius, fluid density and surface tension: $De < 23$, which applies to PEO in the elastic regime II.

de Gans *et al* (2005) examined the role of polymer molecule topology in the formation of ink-jet ligaments, for polymers of the same molecular weight and identical chemistry dissolved in ATP. They used branched "star" and linear poly(methyl methacrylate) (PMMA) , and found that the star polymers could be jetted at higher concentrations than the linear PMMA. The condition Wi > L for extensional viscosity may have applied within their thinning jets. We recall that the onset of regime III is determined by Wi = L. For star polymers, the effective L for a given M_w is significantly reduced, which lowers the Wi threshold. In DoD jetting, star polymers may show regime III behaviour and thus be more readily jettable at higher concentrations and molecular weights.

Under-estimation of relaxation time (Clasen *et al* (2006), Vadillo *et al* (2012)) and over-estimation of extensibility (Szabo *et al* (2012)) both increase the likelihood of the occurrence of regime III behaviour in fast polymer ink-jet printing applications.

V. Conclusions

For the jetting of solutions of polystyrene in good solvents under conditions representative of drop-on-demand ink-jet printing, we have identified three different regimes of behaviour linked to the underlying polymer physics and the jetting conditions, and have presented a quantitative model which shows good agreement with experimental data. Transitions between the regimes occur at critical values of Wi. In regime I (Wi < ½) the polymer chains are relaxed and the fluid behaves in a Newtonian manner. In regime II (½ < Wi < L_1) the fluid is viscoelastic. In regime III (Wi > L_1) the chains remain fully extended in the thinning ligament, a condition which non-intuitively allows more polymer to be jetted at the same speed than if the fluid were behaving elastically. Data reported by de Gans *et al* (2004) are predominantly representative of regimes I and II, while experiments reported here represent regime III. Numerical simulations of jet formation in viscoelastic fluids in drop-on-demand inkjet printing by Morrison and Harlen (2010), which showed the same scaling law as the present experimental data for polystyrene in DEP region III, are now also explained, and shown to relate to regime III. Data from A-Alamry *et al* (2011) on PS and PMMA jetting using other ink-jet print head hardware, display scaling behaviour from regimes I, II and III dependent on the print head drive voltage and hence drop speed in a manner that is consistent with the model. Even under shear conditions appropriate for chain scission, the jetting behaviour with molecular weight appears well predicted. Rheological measurements suggest that this new regime III scaling behaviour should be seen in high speed ink-jet printing of linear polymer solutions.

Acknowledgements

We are grateful to Tri Tuladhar (Department of Chemical Engineering, University of Cambridge) for preparation and characterisation of the polymer master solutions, and to SunJet for supply of the polystyrene. We thank Steve Temple, Mark Crankshaw, Damien Vadillo, John Hinch and Neil Morrison for helpful discussions. The reviewers are thanked for their comments and suggestions to strengthen the original manuscript. The work was supported by the UK Engineering and Physical Sciences Research Council though grant numbers GR/T11920/01 (Next Generation Inkjet Technology) and EP/H018913/1 (Innovation in Industrial Inkjet Technology).

References

A-Alamry, K.; Nixon, K.; Hindley, R.; Odell, J. A.; Yeates, S. G., "Flow-Induced Polymer Degradation During Ink-Jet Printing", *Macromolecular Rapid Communications* **32**, 316-320 (2011)

Anna, S.L. and G.H. McKinley, "Elasto-capillary thinning and breakup of model elastic liquids", *Journal of Rheology* **45**, 115-138 (2001).

Ardekani, A. M.; Sharma, V.; McKinley, G. H., "Dynamics of bead formation, filament thinning and breakup in weakly viscoelastic jets", *Journal of Fluid Mechanics* **665**, 46-56 (2010).

Basaran, O. A., "Small-scale free surface flows with breakup: Drop formation and emerging applications", *Aiche Journal* **48**, 1842-1848 (2002).

Bazilevskii, A. D.; Meyer, J. D.; Rohzkov, A. N., "Dynamics and breakup of pulse microjets of polymeric liquids", *Fluid Dynamics* **40**, 376-392 (2005).

Campo-Deaño, L. and Clasen, C., "The slow retraction method (SRM) for the determination of ultra-short relaxation times in capillary breakup extensional rheometry experiments", *Journal of Non-Newtonian Fluid Mechanics* **165**, 1688-1699 (2010).

Chilcott, M. D. and Rallison, J. M., "Creeping flow of dilute polymer solutions past cylinders and spheres", *J. Non-Newtonian Fluid Mechanics* **29,** 381-432 (1988).

Christanti, Y. and Walker, L.M., "Surface tension driven jet break-up of strain-hardening polymer solutions", *J. Non-Newtonian Fluid Mech.* **100** 9-26 (2001).

Clasen, C.; Plog, J. P.; Kulicke, W. M.; Owens, M.; Macosko, C.; Scriven, L. E.; Verani, M.; McKinley, G. H., "How dilute are dilute solutions in extensional flows?", *Journal of Rheology* **50**, 849-881 (2006).

Cooper-White, J. J.; Fagan, J. E.; Tirtaatmadja, V.; Lester, D. R.; Boger, D. V., "Drop formation dynamics of constant low-viscosity, elastic fluids", *J. Non-Newtonian Fluid Mechanics* **106**, 29-59 (2002).

de Gans, B.-J. and Schubert, U. S., "Ink-jet printing of well-defined polymer dots and arrays", *Langmuir* **20,** 7789–7793 (2004).

de Gans, B.-J.; Kazancioglu, E.; Meyer, W.; Schubert, U. S., “Ink-jet printing polymers and polymer libraries using micropipettes”, *Macromol. Rapid Commun.* **25**, 292–296 (2004).

de Gans, B. J.; Xue, L. J.; Agarwal, U. S.; Schubert, U. S., “Ink-jet printing of linear and star polymers”, *Macromolecular Rapid Communications* **26**, 310-314 (2005).

Entov, V. M. and E.J. Hinch, “Effect of a spectrum of relaxation times on the capillary thinning of a filament of elastic liquid”, *J. Non-Newtonian Fluid Mechanics* **72**, 31-53 (1997).

Goldin, M.; Yerushalmi, J.; Pfeffer, R.; Shinnar, R., “Breakup of a laminar capillary jet of a viscoelastic fluid”, *J. Fluid Mech.* **38**, 689-711 (1969).

Goren, S.L. and M. Gottlieb, “Surface-tension-driven breakup of viscoelastic liquid threads”, *J. Fluid Mech.* **120**, 245-266 (1982).

Graessley, W. W., “Polymer-Chain Dimensions and the Dependence of Viscoelastic Properties on Concentration, Molecular-Weight and Solvent Power”, *Polymer* **21**, 258-262 (1980).

Hinch, E. J., “Mechanical models of dilute polymer-solutions in strong flows”, *Physics of Fluids* **20**, S22-S30 (1977).

Hinch, E. J., “Uncoiling a Polymer Molecule in a Strong Extensional Flow”, *J. Non-Newtonian Fluid Mechanics* **54**, 209-230 (1994).

Hoath, S. D.; Martin, G.D.; Castrejón-Pita, J. R.; Hutchings, I.M., “Satellite formation in drop-on-demand printing of polymer solutions”, Non-Impact Printing *(Society for Imaging Science and Technology, Springfield VA, 2007),* Vol. **23**, 331-335.

Hoath, S. D.; Hutchings, I. M.; Martin, G. D.; Tuladhar, T. R.; Mackley, M. R.; Vadillo, D. C., “Links between ink rheology, drop-on-demand jet formation, and printability”, *J. Imaging Sci. Technol.* **53**, 041208-041208-8 (2009).

Hoyt, J.W.; J. J. Taylor; C.D. Runge, *J. Fluid Mech.* “The structure of jets of water and polymer solution in air”, **63**, 635-640 (1974).

Hsieh, C. C. and Larson, R. G., “Prediction of coil-stretch hysteresis for dilute polystyrene molecules in extensional flow”, *Journal of Rheology* **49**, 1081-1089 (2005).

Hutchings, I. M.; Martin, G. D.; Hoath, S. D., “High speed imaging and analysis of jet and drop formation”, *J. Imaging Sci. Technol.* **51**, 438-444 (2007).

Jung, S.; Hoath, S. D.; Martin, G. D.; Hutchings, I. M., “Experimental study of atomization patterns produced by the oblique collision of two viscoelastic liquid jets”, *J. Non-Newtonian Fluid Mech.* **166**, 297-306 (2011).

McKinley, G. H. and T. Sridhar, “Filament-stretching rheometry of complex fluids”, *Annual Review of Fluid Mechanics*, **34**, 375-415 (2002).

Meyer, J.D.; Bazilevski, A.V.; Rozkov, A. N., “Effects of polymeric additives on thermal ink jets,” in *Recent Progress in Ink Jet Technologies II*, edited by E. Hanson *(Society for Imaging Science and Technology, Springfield VA, 1999)*, Chap. 6, pp. 450-455.

Morrison, N. F. and O.G. Harlen, “Viscoelasticity in Ink-jet Printing”, *Rheologica Acta* **49**, 619-632 (2010)

Mun, R.P.; J.A. Byars; D.V. Boger, “The effects of polymer concentration and molecular weight on the breakup of laminar capillary jets”, J. Non-Newtonian Fluid Mech. **74**, 285–297 (1998).

Somani, S.; Shaqfeh, E. S. G.; Prakash, J. R., “Effect of Solvent Quality on the Coil-Stretch Transition”, *Macromolecules* **43**, 10679-10691 (2010).

Szabo, P.; McKinley, G. H.; Clasen, C., “Constant force extensional rheometry of polymer solutions”, *Journal of Non-Newtonian Fluid Mechanics* **169-170**, 26-41 (2012).

Tirtaatmadja, V.; McKinley, G. H.; Cooper-White, J. J., “Drop formation and breakup of low viscosity elastic fluids: Effects of molecular weight and concentration”, *Physics of Fluids* **18**, 043101 (2006).

Tuladhar, T. R. and M.R. Mackley, “Filament stretching rheometry and break-up behaviour of low viscosity polymer solutions and ink-jet fluids”, *J. Non-Newtonian Fluid Mech.* **148**, 97-108 (2008).

Vadillo, D. C., Hoath, S. D., Hsiao, W.-K. and Mackley, M. R., “The effect of inkjet ink composition and rheology and jetting behaviour”, *Non Impact Printing* (Society for Imaging Science and Technology, Springfield, VA. 2011), Vol. **27**, pp.568-572.

Vadillo, D. C.; Tuladhar, T. R.; Mulji, A.; Mackley M. R., “The rheological characterisation of linear viscoelasticity for ink jet fluids using Piezo Axial Vibrator (PAV) and Torsion Resonator (TR) rheometers”, *Journal of Rheology* **54**, 781-795 (2010).

Vadillo, D. C.; Tuladhar, T. R.; Mulji, A. C.; Jung, S.; Hoath, S. D.; Mackley, M. R., “Evaluation of ink jet fluids performance using the “Cambridge Trimaster” filament stretch and break-up device”, *Journal of Rheology* **54**, 261-282 (2010).

Vadillo, D. C.; Hoath, S.D.; Hsiao, W.-K.; Mackley, M.R., “The effect inkjet ink composition on rheology and jetting behaviour”, *Society for Imaging Science and Technology* Non Impact Printing **27**, 568-572 (2011).

Vadillo, D. C., Mathues, W., Clasen, C., “Microsecond relaxation processes in shear and extensional flows of weakly elastic polymer solutions”, *Rheologica Acta* **50** (2012).

Xu, D.; Sanchez-Romaguera, V.; Barbosa, S.; Travis, W.; de Wit, J.; Swan, P.; Yeates, S. G., “Ink-jet printing of polymer solutions and the role of chain entanglement”, *J. Mater. Chem.* **17**, 4902-4907 (2007).

Yan, X. J.; Carr, W. W.; Dong, H. M. “Drop-on-demand drop formation of polyethylene oxide solutions”, *Physics of Fluids* **23**, 107101 (2011)